Recently, the approaches used to grow long-term lines of T cells have also been applied to B cells. Lines of non-transformed, growth-factor dependent B lymphocytes of mouse[30] and human[31] origin have been propagated for periods of >10 months. The growth of these cells seems to depend on a growth factor produced by T lymphocytes but which is distinct from IL-2 (M. Howard *et al.* and W.E.P., submitted for publication, and B.S., B. Stadler, J. J. Oppenheim and W.E.P., unpublished observations). This factor has been termed B-cell growth factor (BCGF) and studies of its properties are now in progress. B cells grown in long-term culture can be stimulated to secrete immunoglobulin and human B-cell lines have been successfully cloned by limiting dilution.

Potential

We may anticipate that the use of cloned T-lymphocyte populations will be of great value in the functional, molecular and genetic characterization of T-lymphocyte receptors and will lead to a more complete understanding of both the molecular basis and biological significance of histocompatibility restriction. We may also anticipate that a further understanding of the regulatory interactions of immunocompetent cells will come from the preparation of cloned lines of each cell type and from the analysis of the molecules that mediate these interactions. Furthermore, the application of this technology to human T[3,22] and B[30] lymphocytes will have great importance in various clinical situations. Cloned T-cell lines will be valuable as tissue-typing reagents[32] and may have applications in specific therapy for certain infectious agents (J. M. Chiller, personal communication) and tumours[33,34].

Much work remains to be done; it is particularly important to establish the extent to which such long-term cells are 'normal' (that is, how closely they resemble lymphocytes *in vivo*). It seems reasonable to predict that long-term lines of cloned lymphocytes will become standard tools of the cellular immunologist.

1. Ben-Sasson, S. Z., Paul, W. E., Shevach, E. & Green, I. *J. exp. Med.* **141,** 90–105 (1975).
2. MacDonald, H. R., Engers, H. D., Cerottini, J.-C. & Brunner, K. *J. exp. Med.* **140,** 718–730 (1974).
3. Morgan, D. A., Ruscetti, F. W. & Gallo, R. *Science* **193,** 1007–1008 (1976).
4. Möller, G. (ed.) *Immun. Rev.* **51,** 1–357 (1980).
5. Nabholz, M., Engers, H. D., Collavo, D. & North, M. *Curr. Topics Microbiol. Immun.* **81,** 176–187 (1978).
6. Fathman, C. G. & Hengartner, H. *Nature* **272,** 617–618 (1978).
7. Kimoto, M. & Fathman, C. G. *J. exp. Med.* **152,** 759–770 (1980).
8. Sredni, B., Tse, H. Y. & Schwartz, R. H. *Nature* **283,** 581–583 (1980).
9. Nabel, G., Fresno, M., Chessman, A. & Cantor, H. *Cell* **23,** 19–28 (1981).
10. Sredni, B., Tse, H. Y., Chen, C. & Schwartz, R. H. *J. Immun.* **126,** 341–347 (1981).
11. Farrar, J. J., Mizel, S. B., Fuller-Farrar, J., Farrar, W. L. & Hilfilker, M. L. *J. Immun.* **125,** 793–798 (1980).
12. Larson, E. L., Iscove, N. N. & Countinho, A. *Nature* **283,** 664–666 (1980).
13. Mizel, S. B. & Mizel, D. *J. Immun.* **126,** 834–837 (1981).
14. Rosenwasser, L. J., Dinarello, C. A. & Rosenthal, A. S. *J. exp. Med.* **150,** 709–713 (1979).
15. Schmidt, J. A., Mizel, S. B. & Green, I. *Fedn Proc.* **40**(3), 1084 (1981).
16. Smith, K. A. *Immun. Rev.* **51,** 337–357 (1980).
17. Robb, R. J., Munck, A. & Smith, K. A. *J. exp. Med.* **154,** 1455–1474 (1981).
18. Gillis, S., Smith, K. A. & Watson, J. *J. Immun.* **124,** 1954–1962 (1980).
19. Farrar, J. *et al. J. Immun.* **125,** 2555–2558 (1980).
20. Watson, J., Gillis, S., Marbrook, J., Mochizuki, D. & Smith, K. A. *J. exp. Med.* **150,** 849–861 (1979).
21. Piperno, A. G., Vassalli, J. & Reich, E. *J. exp. Med.* **154,** 422–431 (1981).
22. Paul, W. E. & Benacerraf, B. *Science* **195,** 1293–1300 (1977).
23. Sredni, B., Volkman, D., Schwartz, R. H. & Fauci, A. S. *Proc. natn. Acad. Sci. U.S.A.* **78,** 1858–1862 (1981).
24. Sredni, B., Matis, L. A., Lerner, E. A., Paul, W. E. & Schwartz, R. H. *J. exp. Med.* **153,** 677–693 (1981).
25. Fathman, C. G. & Kimoto, M. *Immun. Rev.* **51,** 57–80 (1981).
26. Jones, P. P., Murphy, D. B. & McDevitt, H. O. *J. exp. Med.* **148,** 925–939 (1978).
27. von Boehmer, H. *et al Eur. J. Immun.* **9,** 592–597 (1979).
28. Sredni, B. & Schwartz, R. H. *Nature* **287,** 855–857 (1980).
29. Schwartz, R. H. & Sredni, B. *Isolation, Characterization and Utilization of T Lymphocytes* (eds Fathman, G. & Fitch, F. W.) (Academic, New York, in the press).
30. Howard, M., Kessler, S., Chused, T. & Paul, W. E. *Proc. natn. Acad. Sci. U.S.A.* **78,** 5788–5792 (1981).
31. Sredni, B., Sieckmann, D. G., Kumagai, S. H., Green, I. & Paul, W. E. *J. exp. Med.* **154,** 1500–1516 (1981).
32. Bach, F. H., Alter, B. J., Widmer, M. B., Segall, M. & Dunlap, B. *Immun. Rev.* **54,** 5–26 (1981).
33. Lotze, M. T., Line, B. R., Mathisen, D. J. & Rosenberg, S. A. *J. Immun.* **125,** 1487–1493 (1980).
34. Gillis, S. & Watson, J. *Immun. Rev.* **54,** 81–110 (1981).
35. Gootenberg, J. E., Ruscetti, F. W., Mier, J. W., Gazdar, A. & Gallo, R. C. *J. exp. Med.* **154,** 1403–1418 (1981).

ARTICLES

The 1883 eruption of Krakatau

Stephen Self

Department of Geology, Arizona State University, Tempe, Arizona 85287, USA

Michael R. Rampino

NASA Goddard Institute for Space Studies, Goddard Space Flight Center, New York, New York 10025, USA

The 1883 eruption of Krakatau was a modest ignimbrite-forming event. The deposits are primarily coarse-grained dacitic, non-welded ignimbrite. Large explosions produced pyroclastic flows that entered the sea, generating destructive tsunami. Grain-size studies of the ignimbrite suggest that these explosions were not driven by magma–seawater interaction. The total bulk volume of pyroclastic deposits, including co-ignimbrite ash, is estimated to be 18–21 km^3.

ALTHOUGH the paroxysmal eruption of Krakatau (or Krakatoa) in 1883 was very spectacular there are little data relating to the mechanism of the eruption, or to interpretation of the pyroclastic deposits in terms of modern volcanologic theory. Studies have concentrated on Anak Krakatau, a young cone growing in the 1883 caldera[1], and not on the 1883 deposits. The idea of caldera formation by explosive removal of cone material has been revived[2] but we dispute this mechanism.

We report here results mainly from new field investigations at Krakatau during September 1979. We attempt to correlate the eruption sequence reported previously with the stratigraphy of the deposits to re-evaluate proposed mechanisms for the eruption.

Most interpretations of the Krakatau event rest on the studies of Verbeek[3,4]. He was the first to propose that the huge explosions were caused by seawater coming into contact with the magma within the volcano. Deposits resulting from such phreatomagmatic activity for other eruptions are described elsewhere[5]. Verbeek also suggested that reaction with seawater caused the magma to froth, thus forming the extensive pumice ejected in the 1883 eruption. Although this latter interpretation is now seen to be incorrect, the question of interaction of the magma with seawater as a possible cause of the catastrophic explosions is still being debated[2,6]. However, the eruption is usually ascribed to such phreatomagmatic activity.

Later workers have recognized that the near-source deposits of the 1883 eruption were largely emplaced by pyroclastic flows. Williams and McBirney[7] suggested that these flows may have swept for some distance across the floor of the Sunda Straits. We now present evidence that the culminating event of the Krakatau eruption was the generation of pyroclastic flows by gravitational collapse of the eruption column after several

0028-0836/81/520699—06$01.00

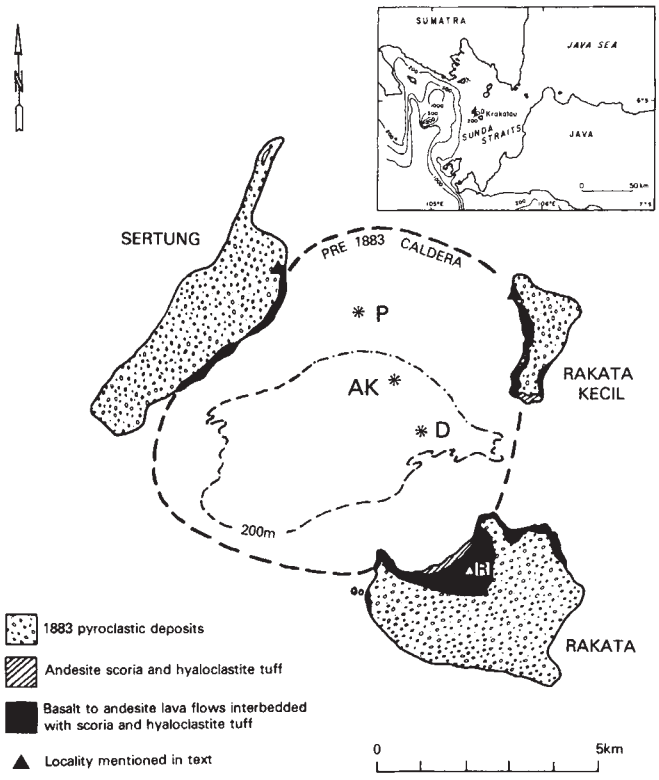

Fig. 1 Sketch map of Krakatau Islands showing prehistoric caldera, possible 1883 caldera outline (200-m isobath, lighter dashed line, dash-dot where conjectural) and simplified geology. R, Rakata cone; P and D are positions of Perbuwatan and Danan vents on pre-1883 Krakatau Island; AK, vent of Anak Krakatau. Outline of islands is from Indonesian Geological Survey map (1940). Inset: location of Krakatau Islands; isobaths in metres (after ref. 2).

large magmatic explosions. We discuss here the role of magma–seawater interaction during the eruption and suggest that the major tsunami that accompanied the eruption were produced when the pyroclastic flows entered the sea.

Before the eruption of 1883, Krakatau consisted of a large island 9 km long and 5 km wide constructed of three volcanoes, Perbuwatan, Danan and Rakata, situated along a fissure within a prehistoric caldera ~7 km in diameter[8]. The surrounding smaller islands of Sertung (formerly Verlaten Island) and Rakata Kecil (Lang Island) are remnants of the rim of the prehistoric caldera (Fig. 1). Krakatau Island largely disappeared during the 1883 eruption, leaving only the southern portion of the cone of Rakata volcano (and a small rock pinnacle) exposed above sea level. The consensus of opinion is that the main vent or vents for the 1883 eruption lay between the vents of Perbuwatan and Danan. Our results are consistent with a vent location in this general area; the location of Anak Krakatau may be controlled by the 1883 vent and conduit.

The foundation of the Krakatau volcano is largely basaltic andesite to andesite composition[9]. The 1883 eruption produced a widespread deposit of non-welded dacitic ignimbrite which covers major portions of the present Rakata, Sertung and Rakata Kecil Islands.

Stratigraphy of the 1883 deposits

We have compared the stratigraphy of the pyroclastic deposits examined in the field with the contemporary eruption records compiled by Verbeek[3,4], and with the later work of Stehn[10] and Williams[8]. The chronology of the eruption, tsunami, stratospheric effects, and the global spread and transport of long residence time 'dust' were documented in the Krakatoa Committee Report of 1888[11].

A composite section of the pyroclastic deposits of the 1883 eruption is shown in Fig. 2. The stratigraphy of the airfall and pyroclastic surge beds is based primarily on two localities on Sertung and Rakata Kecil Islands (Fig. 1), and the stratigraphy of the pyroclastic flow deposits (ignimbrite) is based on several cliff exposures on the western coasts of Rakata and Sertung Islands.

The 1883 eruption began with a period of intermittent mild explosive activity on 20 May 1883. Contemporary reports suggest that on 26 August 1883, at about 13h 00min LT the volcano went into an increasingly explosive phase of eruption, producing a more or less continuous eruption column through explosions at brief intervals (~10 min) (see Judd in ref. 11). The largest explosions during this stage of eruption were recorded at 17h 07 min on the evening of 26 August and 1h 42min, 2h 25min and 4h 43min on 27 August (Fig. 3; see Judd in ref. 11). The eruption column is reported to have been up to 25 km high during this interval. Ships within ~20 km of the volcano reported heavy ash fall, with large pumice clasts (up to ~10 cm diameter) (Judd in ref. 11).

The explosions produced fall units of dacitic pumice up to 20 m thick that are exposed on the islands of Rakata Kecil and Sertung. Pyroclastic surge deposits, found interstratified with the fall units, indicate that minor eruption column collapse during this stage of the eruption produced thin, low-density turbulent pyroclastic surges[12]. All outcrops of the fall/surge deposits are very close to the source (only 2 or 3 km from the supposed vent) and it is inferred that the surges were fairly localized (with much material probably flowing onto or into the sea). The fall deposits were probably of sub-plinian type[13,14] and also of modest dispersal. For example, there were reports of only minor ash fall in southern Sumatra and western Java before the climax of the eruption of 27 August (ref. 11, p. 14). No pumice fall deposits were found beneath pyroclastic-flow and surge deposits on Rakata Island, only 6 km south-east of the vent, even though exposure was excellent. However, the axis of dispersal of the ash fall may have been directed to the west or south-west[4].

On Rakata Kecil Island, an estimated 3 km from the source vent, two uppermost 5–6-m thick pumice fall units are welded to form a dark-grey coherent deposit, differing markedly in colour from the over- and underlying white dacitic pumice (Fig. 4*a*). Sparks and Wright[15] have described similar welded airfall tuffs

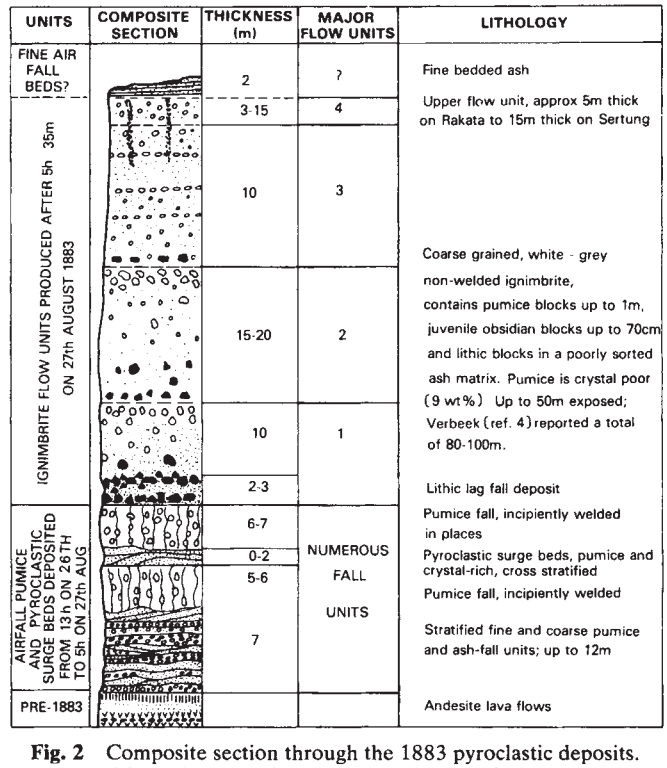

Fig. 2 Composite section through the 1883 pyroclastic deposits. Layers of fine ash at top of section were observed from the boat in cliff sections but were inaccessible to examination in the field.

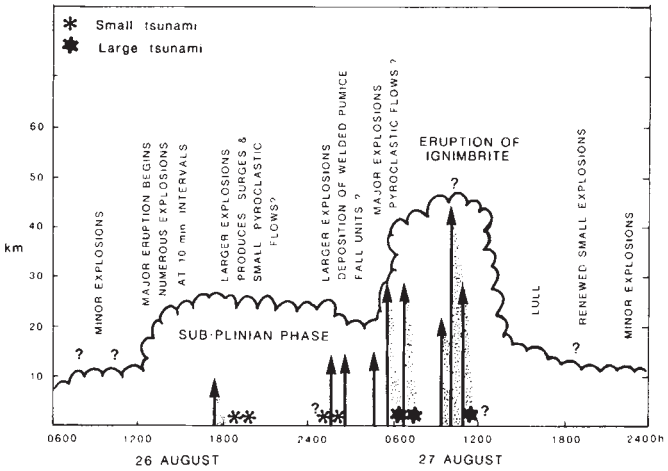

Fig. 3 Sequence of reported explosions and tsunami during 26–27 August 1883 (all times are local). Data from refs 3, 4 and 11. Relative magnitudes of explosions, as recorded by the Batavia gasometer, are indicated by lengths of arrows. Approximate eruption column heights given at left are not accurate to more than ±5 km. Travel times of tsunami from Krakatau to Java and Sumatra coasts estimated at between 30 min and 1 h (ref. 11).

of silicic composition; such tuffs are localized around the vent and indicate high rates of eruption and accumulation of pumice, but imply perhaps only moderate (<2 km) heights for the gas-thrust part of the eruption column. This combination allows the hot, plastic pumice to sinter and agglutinate under its own weight on deposition. Grain-size analyses of the incipiently welded fall unit show it to be rather poorly sorted ($\sigma\phi = 3.2$), and similar to many previously studied non-welded proximal pumice-fall deposits (Fig. 5).

That the pumice-fall deposits are relatively coarse grained compared with phreatoplinian[5] deposits (Fig. 5) suggests that, during the sub-plinian phase of the eruption, the Krakatau explosions were largely magmatic and did not involve significant interaction with seawater. The lithic-poor nature of most of the fall deposits also suggests that, during these early stages of the eruption, large-scale break-up and collapse of the volcanic edifice into the conduit (to allow access of seawater) did not occur. The surge deposits at Krakatau are also lithic poor and similar to the thin pumice-rich ground-surge deposits associated with other ignimbrite-forming eruptions and described from several other localities[16].

At about 5h 30min on 27 August, the style of the eruption changed dramatically (Fig. 3). The first of five enormous explosions took place. Wharton[11] gives the times of the largest explosions as 5h 30min, 6h 44min, 9h 29min, 10h 02min and 10h 52min LT on 27 August; Verbeek[3,4] gives slightly different times (3–5 min later) based on a different reading of the gasometer tracing from Batavia, which fortuitously recorded the air waves from the explosions.

We suggest that each large explosion yielded a pyroclastic flow, almost instantaneously, by large-scale gravitational collapse of the eruption column. These flows moved rapidly off the island and into the sea. The four thick major pyroclastic flow units observed in the field (Fig. 2) probably correspond to the four largest explosions (Fig. 3; see ref. 10).

Material came from the vent between explosions, but was probably finer grained and not of significant volume. We may compare this with the Mt Ngauruhoe, New Zealand eruption sequence of 19 February 1975 (ref. 17) where after an initial period of more or less continuous magma flux, activity declined, then began again with a series of large explosions, each producing a small pyroclastic flow. We propose that the Krakatau eruption sequence was similar but on a much larger scale.

Characteristics of the 1883 ignimbrite

The Krakatau pyroclastic flows apparently moved preferentially to the north and north-east and covered the islands and surrounding sea floor with dacitic ignimbrite (Fig. 6). The biased distribution could be due to directed explosions and/or the topographical control of Rakata volcano (813 m) on the collapsing eruption column, forcing material northwards. The only reports of burns caused by hot ash and gases come from the area around Kalimbang in southern Sumatra, 40 km north-east of Krakatau and 25 km in a direct line from temporary islands produced by the pyroclastic flows. The destruction to the north may have been at the outer edge of a directed blast zone, or perhaps due to ash-cloud surges generated off the tops of moving pyroclastic flows[12]. Such ash-cloud surges can apparently move across water as they did in the St Pierre disaster in 1902[18].

Deposition of ignimbrite extended Sertung and Rakata Kecil Islands and the southern and eastern parts of Rakata (Fig. 6). Shallowing of the sea floor as far as 15 km to the north of Krakatau[3] was caused by submarine pyroclastic flows that

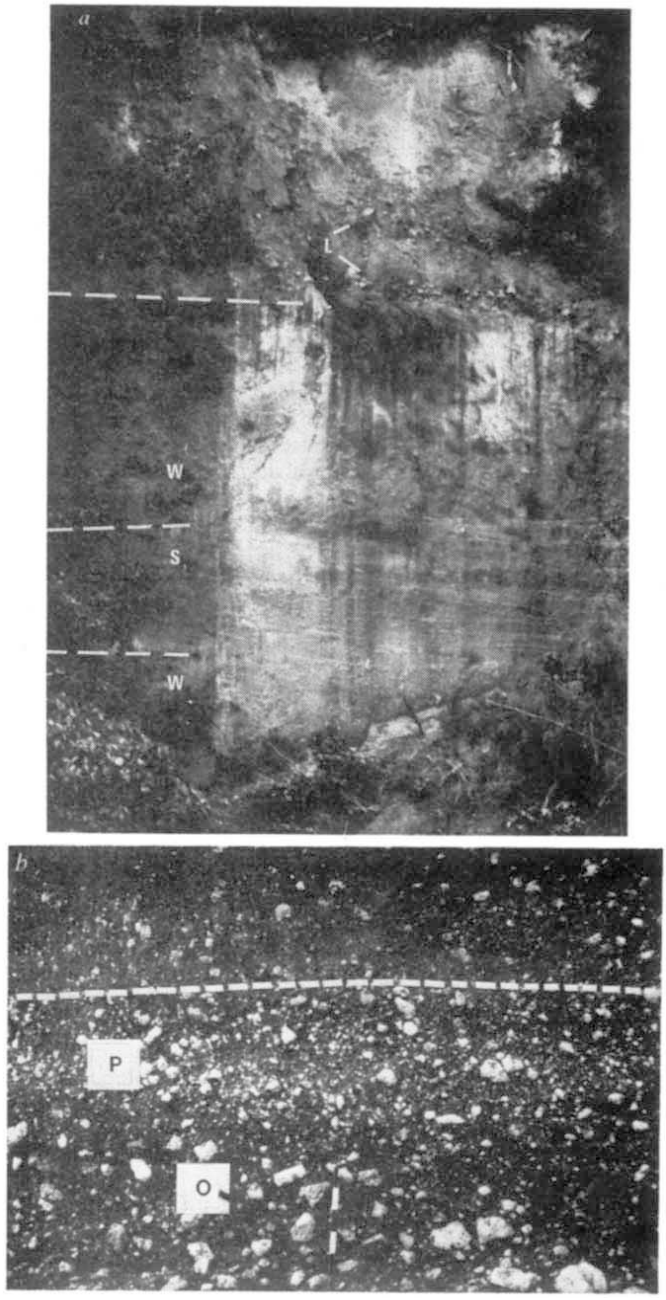

Fig. 4 *a*, Welded pumice (W), pyroclastic surge (S) and lag (L) deposits on Rakata Kecil Island at locality shown in Fig. 1. Cliff section, 15–18 m high. Above and between lag layer is 1883 ignimbrite. *b*, 1883 Ignimbrite exposed on Rakata Island. Dashed lines, flow-unit boundary; P, indicates pumice concentration at top of flow unit; O, juvenile obsidian clast. Scale is 50 cm long with 10 cm bars.

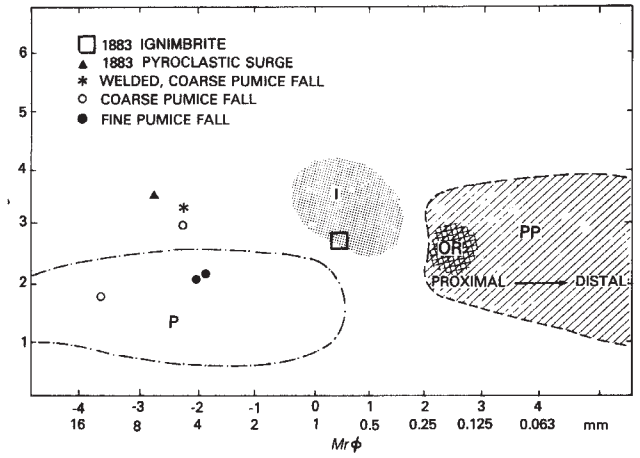

Fig. 5 Grain-size characteristics of Krakatau 1883 pyroclastic deposits, summarized on a plot of median diameter $Md\phi$ ($=\phi_{50}$) against graphical $\sigma\phi$ ($=\sigma_{84}-\sigma_{16}/2$), a sorting parameter. The Krakatau pumice-fall deposits are compared with the field of proximal plinian fall deposits (P) and the field of phreatoplinian deposits (PP), after ref. 5. The Krakatau ignimbrite (plot shows area of four analyses) is compared with the field of normal subaerial ignimbrites (layer 2b in ref. 16), (I) and that of ignimbrite produced from a phreatomagmatic eruption, the Oruanui (Or) ignimbrite (S.S., in preparation).

largely filled the 30–40-m deep basin in the sea floor; two new temporary islands, Steers and Calmeyer Islands, were portions of the ~40-m thick ignimbrite exposed above sea level (Fig. 6). Judd (ref. 11, p. 28) erroneously attributed these pumice banks to the growth of parasitic cones on the flanks of the Krakatau volcano.

Yokoyama[2] suggested that these temporary islands were composed primarily of lithic material derived from the explosive removal of the missing portions of Krakatau Island. However, the field descriptions of Verbeek[3,4] and his chromolithographs of these islands[4] clearly show them to be composed of light-coloured pumice and ash similar to the ignimbrite exposed at Krakatau. The >15 km 'run out' distance of the pyroclastic flows was a result of the vast momentum of several km^3 of pyroclastic debris collapsing from a height of perhaps >5 km (ref. 19).

The 1883 magma was a sparsely porphyritic dacite with ~65–68 wt % SiO_2; the small phenocrysts are plagioclase, augite and minor opaques[4,9]. A small amount (<5 wt %) of grey and white-streaked, mixed pumice is also present.

The ignimbrite is composed of non-welded pumice and ash with ~5 wt % lithic fragments (Figs 2 and 4*b*). A small but significant component (<5 wt % of the deposit) is non-vesiculated to poorly vesiculated obsidian that we consider to be juvenile. The Krakatau ignimbrite has the typical grain-size characteristics of a sub-aerially erupted ignimbrite (Fig. 5). This contrasts with fine-grained phreatoplinian deposits[5] and associated ignimbrites (S.S., in preparation), which were apparently erupted through water. These ignimbrites are much finer grained than the Krakatau ignimbrite, especially in their lack of large-sized components near source (Fig. 5). This again indicates that magma–seawater interaction did not have a significant role in the fragmentation of the magma during the 1883 Krakatau eruption.

Initiation of ignimbrite-forming explosions

Verbeek[3,4] suggested that the Krakatau eruption became submarine at about 10h on 27 August as a result of foundering of the volcanic edifice, and that the largest explosions were caused by seawater rushing into the vent, making contact with the hot magma and causing it to froth explosively into pumice. By contrast, Judd (in ref. 11) argued that entry of large amounts of seawater into the vent would chill the magma and cause it to crust over. Gas would then accumulate below this crust until explosive pressures were reached. These ideas both assume that the volcano was collapsing before the explosions. However, the evidence suggests that this was not the case, and that the subsidence at Krakatau and formation of the caldera took place late in the eruption sequence.

First, lithic debris makes up only ~5% of the deposits which suggests that large-scale collapse of old cone material into the vent was not taking place during the eruption[8]. Second, the coarse-grained nature of both the pumice-fall deposits and the ignimbrite suggests that fragmentation was not caused by magma–seawater interaction. Third, the pyroclastic flow deposits that cover the southeastern part of Rakata Island, and which must have come from one of the vents to the north-west, would be cut off from their apparent source by the caldera wall collapse (Fig. 6). Thus we propose that the large pyroclastic flows were erupted before major collapse of the volcano.

The 1883 caldera lies within the prehistoric Krakatau caldera (~7 km diameter; Fig. 1), and seems to be a graben-like feature extending along two intersecting zones of fractures[8]. The 'missing' portion of the cone of Rakata may represent a large-scale slump of material into the east–west elongated caldera. The >250-m deep caldera was apparently not extensively filled with deposits of 1883 ignimbrite, also suggesting caldera collapse after the eruption of the major pyroclastic flows and emptying of the magma chamber.

We propose that seawater in large quantities did not gain access to the vent during the most explosive stages of the eruption but that seawater may have leaked slowly into the conduit area, sparking small phreatomagmatic explosions. Such explosions would have broken a cap of viscous magma and allowed sudden, explosive release of large batches of vesiculated magma from beneath the upper conduit system (see refs 20–22). Contemporary accounts indicate that the explosive activity subsided in the early hours of 27 August before the large explosions started (Fig. 3). This may have allowed a partly solidified plug to develop in the vent, facilitating the above

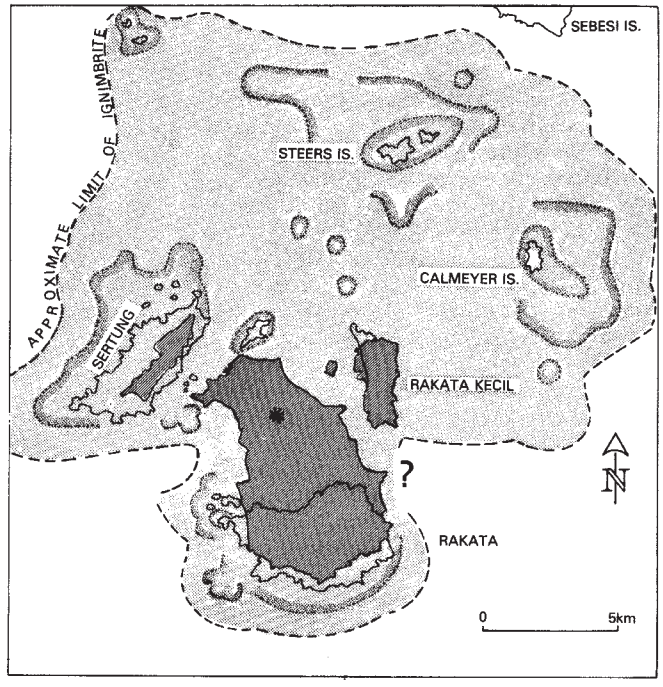

Fig. 6 Submarine distribution of the 1883 ignimbrite, inferred from maps and charts in refs 4 and 11. Hatched area shows outline of the Krakatau Islands before 1883. Stippled pattern shows extent of ignimbrite. Also shown are temporary islands and shallow banks where ignimbrite protruded above sea level (outline of islands after ref. 11).

mechanism. The presence of juvenile obsidian clasts in the ignimbrite might indicate partly solidified magma in the vent.

It has been suggested that some large volcanic explosions can be triggered by magma mixing[23,24]. Sudden mixing of rhyolitic and basaltic or andesitic magma might lead to violent exsolution of dissolved volatiles. A small percentage (<5%) of grey and white-streaked pumice occurs in the Krakatau ignimbrite, suggesting some mixing of magmas. However, we cannot envision a magma-mixing process that would adequately explain the sequence and timing of the large explosions of Krakatau as alluded to by Rice[25]. Magma mixing may have had a role in initiating the eruption, but we do not believe that mixing events were the prime cause of the major explosions on 27 August.

Co-ignimbrite ash

During the eruption of the pyroclastic flows, much vitric dust was dispersed in the atmosphere and formed a widespread thin, fine ash-fall deposit[4]. Considerable distal ash fall did not occur until the large explosions of 27 August, and we suggest that the widespread ash fall was mainly co-ignimbrite ash[26].

Mechanisms envisaged for the generation of the high-altitude column of fine vitric dust and gases that accompanies many events involving production of pyroclastic flows are: (1) rise of selectively fine (low terminal fall velocity) material above the vent; (2) generation of ash from the moving pyroclastic flows; and (3) secondary explosions that may occur as hot pyroclastic flows enter the sea[6]. Evidence for this type of secondary explosion was not found at Krakatau, possibly because of the lack of lateral exposure. However, the expected airfall layers produced by such secondary explosions are not present between the ignimbrite flow units at Krakatau in the outcrops we examined.

All large ignimbrite eruptions are accompanied by the production of co-ignimbrite ash[26]. This fine ash consists of the vitric component—pumice shards and fragmented shards commonly from 50 μm down to a few μm in diameter. The finest ash was capable of significant stratospheric residence times varying from days to months (depending on size). This dust may have been partly responsible for the widespread atmospheric optical phenomena observed after the August 1883 eruption (refs 27, 28, Russell and Archibald in ref. 11), although the sulphate aerosols generated by the eruption were probably more important[29].

Volume of the 1883 eruption

Calculations of the total volume of ejecta from the 1883 eruption must include the volume of widely dispersed dust and ash as well as the subaqueous ignimbrite. Volumetric estimates range widely from Verbeek's 18 km^3 for the total ejecta[3,4], to the Royal Society's value of 14.4 km^3 for the fine distal ash fall alone[11], to recent estimates of 13 ± 4 km^3 (ref. 2) and only 5 km^3 (ref. 30) for the total ejecta based on the volume of the caldera.

Close to Krakatau, Verbeek[4] estimated from field investigations and depth soundings of the sea bottom before and after the eruption that 12 km^3 (bulk volume) was ejected. This is a reasonable figure for the volume of ignimbrite produced, based on a sheet of ignimbrite averaging ~40 m thick and covering an area of ~300 km^2 (Fig. 6). Verbeek also considered the volume of widely dispersed ash and estimated this to be 6 km^3. This value must be a minimum because it only considers a portion of the total dispersal area, which the Krakatoa Committee estimated to be 1.1×10^6 $miles^2$ (see ref. 11, p. 448). Our recalculation of the volume of widely dispersed ash from data in ref. 4, using an area against thickness plot and extrapolating to 1 mm thickness[31], gives 8.5 km^3. Recent studies of co-ignimbrite ash volumes compared with the volume of the parent ignimbrite indicate that up to 50% of the magma erupted can be co-ignimbrite ash[26,32]. Applying the methods for estimating crystal concentration in ignimbrites[26,33], preliminary studies suggest that the Krakatau ignimbrite must have lost at least 40% of the vitric component into the fine co-ignimbrite ash, which therefore has a minimum volume of ~5 km^3. The above calculations suggest a bulk volume of fine, dispersed ash between ~5 km^3 and 8.5 km^3.

The pre-27 August sub-plinian fall and surge deposits are thought to be of small volume, probably <1 km^3. Analysis of samples suggests that only 8% of fine vitric material in these deposits is missing. Therefore, the volume of fine ash produced during the sub-plinian phase of the eruption is very small compared with that emitted during the ignimbrite-forming phase. When the amounts of ignimbrite, co-ignimbrite ash and sub-plinian deposits are added up, the total bulk volume of the 1883 Krakatau deposits is 18–21 km^3. The equivalent volume of dense rock may be roughly estimated as 9–10 km^3.

Generation of tsunami

The Krakatau eruption also produced tsunami that inundated coastal areas around the Sunda Straits. These tsunami are generally attributed to submarine explosions or to caldera collapse[8,34] although ejecta falling into the sea has also been suggested[3,4,11]. The evidence indicates that the tsunami were caused by several cubic kilometres of pyroclastic flow material entering into the sea immediately after each of the large explosions.

The early small explosions of 26 August were followed by small tsunami (Fig. 3). For example, an explosion occurred at about 17h 20min on 26 August, and the first destructive waves reached the Java and Sumatra shores 40 km from Krakatau soon afterwards, between 18h and 19h. This early wave or waves may have been due to surges or small pyroclastic flows entering the sea. No other destructive waves were observed until the morning of 27 August (Wharton, in ref. 11). At about 6h 30min a large wave swept over much of the Java coast; another wave followed at about 7h 30min. At about the same time a wave hit low-lying areas of Sumatra. These waves followed the large explosions at 5h 30min and 6h 44min (Fig. 3).

At some time after 10h a gigantic wave (or waves) inundated the coasts bordering the Sunda Straits. This wave is reported to have been the largest, and was the last recorded in the straits; most survivors of the earlier waves had by this time fled from the coastal areas. The tide gauge at Batavia (Jakarta) also recorded waves that correspond to the large explosions.

The sequence and timing of tsunami suggest that the major tsunami were generated at the times of the explosions (Wharton, in ref. 11). Pyroclastic flows resulting from column collapse would have entered the sea within about ~30 s of the explosions[19] and initiated the tsunami. The slumping of large parts of the volcano, for example the segment of Rakata cone that probably slid into the caldera, could have been a factor in generating tsunami late in the eruption.

The idea that tsunami can be caused by pyroclastic flows entering the sea is supported by a study of the huge eruption of Tambora in 1815 during which tsunami were generated which flooded the nearby coasts of Sumbawa to a height of 4 m, and Java to a height of 2 m (ref. 33). These waves could not have been produced by magma–seawater interactions or caldera collapse, as the volcanic crater lies some 15–20 km inland at an elevation of about 2,850 m. Pyroclastic-flow deposits from the 1815 eruption entered the sea at the base of the volcano (M.R.R. and S.S., in preparation), and this was the most likely cause. The large tsunami that are inferred to have accompanied the Minoan eruption of Santorini[34] may have been generated in the same way.

We conclude that the 1883 eruption was an ignimbrite-forming event of modest volume. The deposits are largely coarse-grained non-welded dacitic ignimbrite and show little support for a phreatomagmatic origin. The occurrence of welded pumice-fall deposits beneath the ignimbrite also seems to argue against water–magma interaction in the early stages of the eruption. The presence of mixed pumice clasts indicates some magma mixing and supports the contention that welded airfall deposits result, in some cases, from superheating of

magma during a mixing event[15].

During the paroxysmal phase, four or five large-volume explosions driven by magmatic gases led to collapse of the eruption column, and to the production of pyroclastic flows that entered the sea. The blasts and ensuing pyroclastic flows seem to have been directed preferentially towards the north and north-east. The times of the explosions correlate with the times of tsunami generation, and we propose that the entry of the pyroclastic flows into the sea caused the major tsunami. Caldera collapse probably came late in the eruption.

The total volume of the deposits of the Krakatau eruption is estimated to be 18–21 km^3 (bulk volume), including 12 km^3 of ignimbrite and up to 8.5 km^3 of distal co-ignimbrite ash fall. When compared with prehistoric ignimbrite-forming events, ranging in volume up to 10^3 km^3 (refs 35, 36), the volume of the Krakatau eruption was very modest.

We thank Adjat Sudradjat and Rudi Hadisantono of the Indonesian Volcanological Survey, Bandung, for their support and assistance. G. P. L. Walker critically reviewed the paper, and J. V. Wright supplied useful ideas and constructive criticism. This work was supported by NASA grant NSG 5145. M.R.R. was a National Academy of Sciences Research Associate during this study. We thank the Indonesian Institute of Sciences (LIPI) for permission to work at Krakatau.

Received 29 July; accepted 20 October 1981.

1. Decker, R. W. & Hadikusumo, D. *J. geophys. Res.* **66**, 3467–3511 (1961).
2. Yokoyama, I. *J. Volcan. geotherm. Res.*, **9**, 359–378 (1981).
3. Verbeek, R. D. M. *Nature* **30**, 10–15 (1884).
4. Verbeek, R. D. M. *Krakatau* (Imprimerie de l'Etat, Batavia, 1886).
5. Self, S. & Sparks, R. S. J. *Bull. volcan.* **41-3**, 1–17 (1978).
6. Walker, G. P. L. *Nature* **281**, 642–646 (1979).
7. Williams, H. & McBirney, A. R. *Geologic and Geophysical Features of Calderas* (Center for Volcanology, University of Oregon, 1968).
8. Williams, H. *Calderas and their Origin* Vol. 25 (Bull. Dept Geol. Sci., University of California, Berkeley, 1941).
9. Westerveld, J. *Bull. geol. Soc. Am.* **63**, 561–594 (1952).
10. Stehn, C. Ch. in *Proc. 4th Pacific Sci. Congr*, Batavia **I**, 1–55 (1929).
11. Symons, G. J. (ed.) *The Eruption of Krakatoa and Subsequent Phenomena* (Rep. Krakatoa Committee of the Royal Society, Trübner, London, 1888).
12. Fisher, R. V. *J. Volcan. geotherm. Res.* **6**, 305–218 (1979).
13. Walker, G. P. L. *Geol. Rdsh.* **62**, 431–446 (1973).
14. Self, S. *J. geol. Soc.* **132**, 645–666 (1976).
15. Sparks, R. S. J. & Wright, J. V. *Geol. Soc. Am. spec. Pap.* **180**, 155–166 (1979).
16. Sparks, R. S. J., Self, S. & Walker, G. P. L. *Geology*, **1**, 115–118 (1973).
17. Nairn, I. A. & Self, S. *J. Volcan. geotherm. Res.* **3**, 39–60 (1978).
18. Fisher, R. V., Smith, A. L. & Roobol, M. J. *Geology* **8**, 472–476 (1981).
19. Sparks, R. S. J., Wilson, L. & Hulme, G. *J. geophys. Res.* **83**, B4, 1727–1739 (1978).
20. Schminke, H.-U. *Geol. Jb.* **A39**, 3–45 (1977).
21. Self, S., Wilson, L. & Nairn, I. A. *Nature* **277**, 440–443 (1979).
22. Wilson, L. *J. Volcan. geotherm. Res.*, **8**, 297–313 (1980).
23. Sparks, R. S. J., Sigurdsson, H. & Wilson, L. *Nature* **267**, 315–323 (1977).
24. Eichelberger, J. C. *Nature* **275**, 21–27 (1978).
25. Rice, A. *J. geophys. Res.* **86**, 405–417 (1981).
26. Sparks, R. S. J. & Walker, G. P. L. *J. Volcan. geotherm. Res.* **2**, 329–341 (1977).
27. Wexler, H. *Bull. Am. met. Soc.* **33**, 48–51 (1951).
28. Deirmendjian, D. *Adv. Geophys.* **16**, 267–297 (1973).
29. Hansen, J. E., Wang, W.-C. & Lacis, A. A. *Science* **199**, 1065–1068 (1978).
30. Kent, D. V. *Science* **211**, 648–650 (1981).
31. Walker, G. P. L. *J. Volcan. geotherm. Res.* **8**, 69–94 (1980).
32. Sparks, R. S. J. & Huang, T. C. *Geol. Mag.* **117**, 425–436 (1980).
33. Walker, G. P. L. *Contr. Mineral. Petrol.* **136**, 135–146 (1972).
34. Neumann Van Padang, M. *Acta of the 1st International Scientific Congress on the Volcano Thera*, 51–63 (Archaeological Service of Greece, Athens, 1971).
35. Smith, R. L., *Geol. Soc. Am. Spec. Pap.* **180**, 5–24 (1979).
36. Ninkovich, D., Sparks, R. S. J. & Ledbetter, M. T. *Bull. volcan.* **41**, 1–13 (1978).

Evaluation of the Seasat wind scatterometer

W. L. Jones*, D. H. Boggs†, E. M. Bracalente*, R. A. Brown‡, T. H. Guymer§, D. Shelton† & L. C. Schroeder*

* NASA Langley Research Center, Hampton, Virginia 23665, USA
† Jet Propulsion Laboratory, Pasadena, California 91103, USA
‡ University of Washington, Seattle, Washington 98195, USA
§ Institute of Oceanographic Sciences, Wormley, Surrey GU8 5UB, UK

Surface wind velocities have been derived from backscatter measurements of the ocean surface made by a satellite-borne, microwave sensor. Comparisons with high-quality surface-based measurements obtained during the Joint Air–Sea Interaction experiment are described. The accuracy of the scatterometer winds at this mid-latitude site, ±1.6 m s^{-1} in speed and ±18° in direction, for winds between 3 and 16 m s^{-1} is within the design specification.

THE Seasat-A Satellite Scatterometer (SASS) was one of several microwave remote sensors onboard the first oceanographic satellite[1], Seasat-A, and provided wind velocity estimates over the world's oceans from a height of 800 km. The technique is based on the sensitivity of microwave radar backscatter to the amplitude of short gravity waves (few centimetres) created on the sea-surface by the action of the wind. The sensor and the algorithms used to convert radar backscatter into winds are detailed elsewhere[2–5].

Design specifications for the SASS required a wind speed measurement range of 4–26 m s^{-1} with an accuracy of ±2 m s^{-1} or 10% (whichever is the greater) and a wind direction range of 0–360° with an accuracy of ±20°. To check whether these criteria are satisfied the inferred wind vectors must be compared with those obtained by surface instrumentation. Because the accuracy and coverage of routine wind reports at sea are generally not high enough to evaluate the scatterometer measurements properly, a special series of measurements from ships and buoys was conducted in the Gulf of Alaska[6]. It was also fortunate that the field phase of the Joint Air–Sea Interaction (JASIN) experiment[7] took place during the lifetime of Seasat. One of its aims was to provide accurate estimates of the surface meteorological fields over a 200 × 200 km area, and, as a result of careful intercalibrations, high-quality surface wind data are therefore available. This article describes the results of comparisons made at the Seasat–JASIN workshop[8] and demonstrates that the specifications for the SASS have been met for wind speeds up to 16 m s^{-1}.

Seasat scatterometer

The strength of the radar backscatter (normalized radar cross-section σ^0) is a function of the amplitude of very short gravity waves which is itself proportional to the near-surface wind speed. Further, the radar backscatter is anisotropic, so that wind direction can be derived from scatterometer measurements at different azimuths.

The SASS was designed to view the ocean at two azimuths, as shown in Fig. 1. Four dual-polarized, fan-beam antennas were aligned such that they pointed ±45° and ±135° in azimuth relative to the subsatellite track to produce an X-shaped pattern of illumination on the Earth. In this way, a given surface location was viewed first by the forward antenna and then ~1–3 min later (depending on whether the location was at the inner or outer portion of the swath) it was viewed orthogonally by the aft beam. Twelve Doppler filters were used to subdivide the antenna footprint electronically into resolution cells ~15 km (across beam) ×70 km (along beam). In the results presented here pairs of cells were selected having separations <37 km. It is assumed that during the interval between samples the short gravity-wave field integrated over such areas remains constant. The incidence

0028–0836/81/520704—04$01.00